Analyst

ROYAL SOCIETY OF CHEMISTRY

PAPER

View Article Online
View Journal | View Issue

Cite this: *Analyst*, 2025, **150**, 1541

One-pot synthesized three-way junction based multiple strand displacement amplification for sensitive assay of H5N1 DNA†

Zhengjiang Wu,[a,b] Jingwen Li,[b] Tao Zhang,[b,e] Kai Zhang,[c] Xiaomei Liu,[b] Zhan Yang,[d] Li Xu*[a] and Kun Han *[b]

The rapid and sensitive detection of H5N1, a highly pathogenic avian influenza virus, is crucial for controlling its spread and minimizing its impact on public health. In this study, we developed a novel biosensor based on strand displacement amplification (SDA) coupled with CRISPR/Cas12a for highly sensitive detection of H5N1 DNA. The biosensor utilizes a combination of a three-way junction structure, composed of three hairpins (H1, H2, H3), to initiate amplification through SDA, resulting in the production of numerous activators. These activators then trigger CRISPR/Cas12a's collateral cleavage activity, which generates a detectable fluorescence signal. The biosensor demonstrated a linear detection range from 100 fM to 800 pM, with a detection limit as low as 72.87 fM. The optimized biosensor exhibited excellent sensitivity, high specificity, and a broad dynamic range, making it a promising tool for the early detection of H5N1 DNA in complex biological samples. Additionally, the use of CRISPR/Cas12a's trans-cleavage activity significantly improved signal amplification and specificity, allowing for more reliable detection compared to traditional methods. The results highlight the advantages of the integrated SDA and CRISPR/Cas12a approach, which addresses the limitations of conventional detection methods, such as low sensitivity, lengthy analysis times, and high costs. The biosensor's ability to perform well in complex sample matrices demonstrates its potential for point-of-care diagnostics, especially in resource-limited settings. Future applications of this technology could extend to the detection of other pathogens, offering a versatile and adaptable platform for disease surveillance and management.

Received 29th December 2024,
Accepted 11th February 2025

DOI: 10.1039/d4an01586j

rsc.li/analyst

1. Introduction

The H5N1 subtype of influenza A virus is highly lethal and virulent, making it a significant pandemic threat.[1–7] This virus has caused numerous outbreaks among avian populations and has also been transmitted to humans, leading to severe respiratory illness with a high fatality rate. The zoonotic potential of H5N1 and its ability to evolve into more transmissible forms underscore the importance of continuous surveillance and rapid response. Rapid and sensitive detection of H5N1 is essential for controlling its spread and minimizing its impact on public health, particularly in regions with limited access to healthcare infrastructure. Several methods have been developed for H5N1 virus detection, including enzyme-linked immunosorbent assay (ELISA),[8] reverse transcription polymerase chain reaction (RT-PCR),[9–11] surface plasma resonance (SPR),[12] and western blot assay (WB).[13] ELISA is widely used due to its ability to detect viral antigens with moderate sensitivity, but it requires well-prepared samples and multiple washing steps, making it labor-intensive. RT-PCR, on the other hand, remains the gold standard for viral RNA detection due to its high specificity and sensitivity. However, RT-PCR is highly dependent on specialized equipment and skilled technicians, which limits its feasibility in low-resource environments. SPR and WB assays are also effective for specific detection, but both require expensive reagents and instruments, making them unsuitable for widespread field deployment. These traditional methods are often limited by cumbersome sample preparation, lengthy analysis times, high equipment costs, and limited sensitivity, which restrict their practical application in field settings. The need for simpler, more cost-effective, and rapid diagnostic tools has driven the development of novel approaches that can overcome these limit-

[a]*School of the Life Sciences, Jiangsu University, Zhenjiang 212013, China. E-mail: lxu66@ujs.edu.cn*
[b]*Suzhou Institute of Biomedical Engineering and Technology, Chinese Academy of Science, Suzhou 215163, P.R. China. E-mail: hank@sibet.ac.cn*
[c]*School of Chemistry and Materials Science, Nanjing University of Information Science and Technology, Nanjing 210044, P. R. China*
[d]*Huadong Medical Institute of Biotechniques, Nanjing 210018, China*
[e]*Jinan Guoke Medical Technology Development Co., Ltd, Jinan 250101, China*
† Electronic supplementary information (ESI) available. See DOI: https://doi.org/10.1039/d4an01586j

ations. Furthermore, the ability to detect H5N1 at early stages of infection or in asymptomatic carriers is crucial for effective containment, as early diagnosis enables timely intervention to prevent large-scale outbreaks.

To address these problems, several nucleic acid isothermal amplification approaches have been developed, including recombinant polymerase amplification (RPA),[14–18] hybridization chain reaction (HCR),[19,20] catalytic hairpin assembly technique (CHA),[21–27] exponential amplification reaction (EXPAR),[28] rolling loop amplification reaction (RCA),[29–33] DNA Walker,[34,35] loop-mediated isothermal amplification reaction (LAMP),[36] and Strand displacement amplification (SDA)[37–41] *etc*. Among them, SDA is particularly effective for amplifying nucleic acid signals. In typical SDA reactions, the priming sequence initiated by a target-mediated hybridization event extends along a pre-designed template, allowing pre-hybridized targets or newly generated DNA fragments to be displaced, which subsequently triggers further SDA cycles. Despite its effectiveness, SDA suffers from issues such as signal variability and loss, which compromise the consistency and reliability of the results. To overcome these limitations, SDA is often combined with CRISPR/Cas systems, which enhance specificity and sensitivity through collateral cleavage activity, providing an additional layer of signal amplification and reducing false-positive rates. For example, Chi, Z describes the detection of microRNAs using the SDA method without the need for reverse transcription.[37] Zhou, S reported that the SDA method was successfully employed to detect DNA methylation with high sensitivity, demonstrating its suitability for applications requiring precise quantification.[39] These examples illustrate the versatility and effectiveness of SDA in different nucleic acid detection scenarios. However, despite the numerous benefits of the SDA method, it possesses inherent limitations. One challenge with SDA is the potential loss of signal due to variability in reaction products, which can affect consistency and accuracy, particularly in complex sample matrices.

Clustered regularly interspaced short palindromic repeats and their associated Cas proteins (CRISPR/Cas) are essential components of the host's prokaryotic adaptive immune system, providing defense against viral infections.[42] Over the years, the CRISPR/Cas system has been repurposed as a powerful tool for precise genome editing and programmable gene expression control, revolutionizing biotechnology, medicine, and other fields.[43,44] Among the Cas proteins, Cas12a is particularly noteworthy due to its remarkable collateral cleavage activity, which enables its use in the construction of highly sensitive and specific nucleic acid detection platforms for clinical diagnostics.[45–47] The most significant advantage of Cas12a lies in its ability to recognize specific DNA targets and activate a trans-cleavage mechanism that cleaves surrounding non-target DNA, amplifying the detection signal. This lateral cutting activity is a core feature of diagnostic systems such as DNA Endonuclease Targeted CRISPR Trans Reporter (DETECTR) and Cas14-DETECTR, where Cas12a enables highly sensitive detection by generating strong fluorescent signals upon recognition of the target.[48–50] Additionally, Cas12a forms complexes with CRISPR RNA (crRNA), which further enhances its specificity and efficiency in targeting and cleaving DNA. Another major benefit of CRISPR/Cas12a is its ability to detect single-stranded DNA without the need for a protospacer adjacent motif (PAM) site. This flexibility expands its diagnostic potential, allowing for the recognition of a wide variety of genetic sequences, which makes it highly adaptable for detecting diverse pathogens and genetic markers.[51] Cas12a's ability to work with single-stranded DNA is a crucial advantage for applications that require the detection of short or fragmented DNA sequences, such as those found in viral infections or genetic disorders. However, while CRISPR/Cas12a offers tremendous sensitivity and specificity, a single CRISPR-based assay may still face challenges when detecting low-abundance targets, particularly in complex samples. This limitation can be mitigated through the integration of nucleic acid pre-amplification techniques, such as SDA, which significantly enhances the detection sensitivity, allowing for the identification of targets at much lower concentrations. The combination of CRISPR/Cas12a with amplification methods like SDA makes it a powerful tool for reliable, high-sensitivity diagnostics in clinical and field settings.

In this study, based on strand displacement amplification and CRISPR/Cas12a, we developed an H5N1 biosensor. The hairpin H1 was designed for recognizing H5N1 DNA and was assembled with hairpin H2 and H3 to form a three-way junction (TWJ), which enabled the production of numerous activators through strand displacement amplification, the CRISPR/Cas12a system was optimized and assembled using a single-chain structure to activate CRISPR/Cas12a's lateral cleavage activity. The sensor demonstrated excellent analytical sensitivity and high performance in serum samples, offering a valuable reference for real sample applications.

2. Materials and methods

2.1 Material and instruments

All oligonucleotides were obtained from Sangon Biotech (Shanghai, China) and were HPLC purified. The sequences of oligonucleotides are listed in Table S1.† Klenow fragment polymerase *exo-* (5000 U mL^{-1}), dNTP Mixture (2.5 mM) were obtained from Beyotime Biotechnology (Shanghai, China). LbCas12a (100 μM), 10× NEB buffer 2.0, Nt. BbvCI (10 000 U mL^{-1}), 10× Cutsmart buffer were obtained from New England Biolabs (Beijing, China). Recombinant RNase Inhibitor (RRI) was obtained from TaKaRa (Beijing, China). DEPC water and 6× loading buffer were obtained from Sangon Biotech (Shanghai, China). Gel-Red Stain was obtained from KeyGEN BioTECH (Nanjing, China). DNA Marker (10–300 bp) was ordered from Thermo Scientific (Shanghai, China). Reverse Transcription Kit (with gDNase) was obtained from biosharp (Beijing, China). Real samples was obtained from Huadong Medical Institute of Biotechniques (Nanjing, China). Other chemicals were of analytical grade and used without further purification. All solutions were prepared with double distilled water (18 MΩ cm^{-1}) from a Milli-Q purification system (Millipore Corp, Milford, MA) and stored at 4 °C.

Fluorescence spectra were recorded on an F97 fluorescence spectrometer (Shanghai, China). Electrophoresis analysis was conducted using a Tanon electrophoresis analyzer (Tanon 2500R, Shanghai, China).

2.2 Procedure for H5N1 DNA detection

To anneal hairpins, H1, H2, H3 was denatured at 95 °C for 5 min, and then gradually cooled to room temperature. Initially, Cycle 1 and Cycle 2 were formed. The Cycle 1 and Cycle 2 reaction system (10 μL) comprised 1 μL of target solution at various concentrations and 1 μM of each H1, H2 and H3, which reacted at 37 °C for 40 min. Then 1 U μL^{-1} Klenow fragment polymerase *exo-* (KF *exo-*) and 1 U μL^{-1} Nt. BbvCI were added for 30 min at 37 °C, followed by inactivation at 75 °C for 6 min. The Cycle 1 and Cycle 2 system was performed in 1× NE buffer 2.1 (50 mM NaCl, 10 mM Tris-HCl, 10 mM $MgCl_2$, 100 μg mL^{-1} BSA, pH 7.9) Finally, the CRISPR/Cas12a system was performed in 10× NEB buffer 2.0 by adding 4 μL amplification product, 2 μM Cas12a, 1 μM crRNA, 1 μM reporters, and 1 U RRI. The solution (10 μL) was incubated at 37 °C for 35 min. Then 190 μL ddH_2O was mixed with the reaction mixture, and the blend was immediately transferred to a micro colorimetric dish for fluorescence signal detection under 480 nm excitation light and 520 nm emission light. The bandwidths of both excitation and emission were set at 5 nm. The photomultiplier tube voltage was set as 600 V.

2.3 Gel electrophoresis verification analysis

The feasibility of the assay was investigated using 15% polyacrylamide gel electrophoresis (PAGE). The gel was immersed in 1× TBE buffer and run for 60 min at 120 V. It was stained with Gel-Red Stain and imaged using a UV transilluminator (Bio-Tanon, Shanghai, China).

2.4 Detection of H5N1 DNA in fetal bovine serum (FBS)

FBS was diluted 100-fold with 1× NE buffer 2.1 and then different concentrations of H5N1 were added to 1% FBS. H5N1 detection in 1% FBS samples was then carried out using the method.

2.5 Apply to real samples

To explore the method's potential in complex biological samples, the method was used to detect the DNA of H5N1-inactivated virus. H5N1 inactivated virus samples were lysed at 121 °C for 30 min followed by centrifugation at 12 000 rpm for 10 min to obtain the supernatant. Then 1μL of the supernatant was added, 4 μL of 5× RT MasterMix, 1 μL of 20× Oligo dT & Random Primer were added, and then RNase free H_2O was supplemented to 10 μL for 30 minutes. Finally, 1 μL was analyzed using the method.

3. Results and discussion

3.1 The principle of the method

The principle of the strand displacement amplification (SDA) based CRISPR/Cas12a sensing system for H5N1 DNA detection is illustrated in Scheme 1. The sequences of all nucleic acids used are listed in Table S1.† The detection process begins with the hybridization of H5N1 DNA to hairpin H1, which leads to the opening of H1's stem-loop structure, exposing sequences that can bind to the next hairpin in the cascade. Upon binding, the opened H1 hybridizes with hairpin H2, which causes the opening of H2. This is a critical step, as it enables further interaction with hairpin H3. When H3 binds to the now open H2, it displaces the H5N1 DNA because the H1/H3 double-stranded structure has a higher binding affinity and greater thermodynamic stability compared to the H5N1 DNA/H1 structure. This displacement releases the H5N1 DNA, allowing it to re-enter the cycle and initiate another reaction with an additional H1 molecule, effectively generating multiple three-way junctions (TWJ). This repeated cycle is termed Cycle 1, where numerous TWJs are produced, greatly amplifying the signal. Once Cycle 1 is complete, Cycle 2 begins. In Cycle 2, the TWJ structures act as primer-template junctions that drive strand displacement amplification (SDA). This step is facilitated by the action of Klenow fragment polymerase (KF *exo-*) and the nicking enzyme Nt.BbvCI. Klenow fragment polymerase initiates DNA synthesis at the primer-template junction, while Nt.BbvCI introduces specific nicks in the double-stranded DNA, creating entry points for subsequent strand displacements. These processes—extension, nicking, and strand release—are repeated in multiple cycles, resulting in the exponential production of activators. The produced activators then pair with the CRISPR RNA (crRNA), forming an active CRISPR/Cas12a complex. The Cas12a enzyme, once activated, exhibits non-specific single-stranded DNase activity. This activity is crucial for the detection mechanism, as it results in the collateral cleavage of surrounding single-stranded DNA (ssDNA) probes labeled with a fluorophore and a quencher (FQ signal molecule). Upon cleavage, the fluorophore is separated from the quencher, resulting in the release of a strong fluorescence signal. This fluorescence can be easily measured, providing a quantitative readout that indicates the presence of H5N1 DNA. The combination of SDA for target amplification and CRISPR/Cas12a for signal transduction ensures a highly sensitive and specific detection system, capable of identifying even low concentrations of H5N1 DNA in complex biological samples.

3.2 Feasibility of the H5N1 DNA detection

The feasibility of the method for H5N1 DNA detection was verified using both gel electrophoresis and fluorescence tests. In Scheme 1 and Fig. S1,† three metastable stem-loop hairpins were designed with partial complementarity. As illustrated in Fig. 1A, distinct bands corresponding to hairpins H1, H2, and H3 are observed in lanes 1, 2, and 3, respectively, indicating the successful formation of individual hairpins. Lane 4 demonstrates the hybridization between H5N1 DNA and hairpin H1. When H5N1 DNA was introduced into a mixture of H1, H2, and H3, the brightness of the original hairpin bands decreased, and four bright bands with varied mobility appeared in lane 5, and a lighter band above the TWJ likely resulted from a chain reaction between open hairpin H2 and

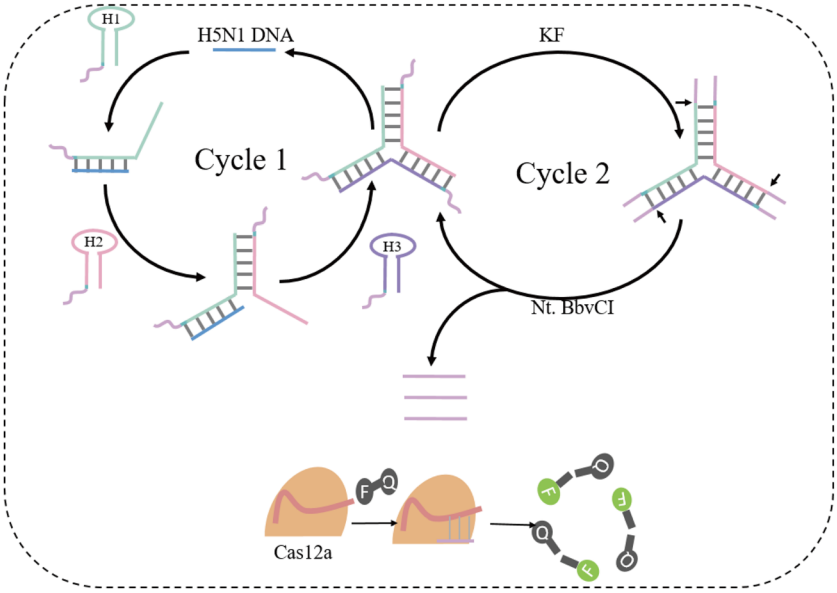

Scheme 1 Schematic diagram of the method for detecting H5N1 DNA.

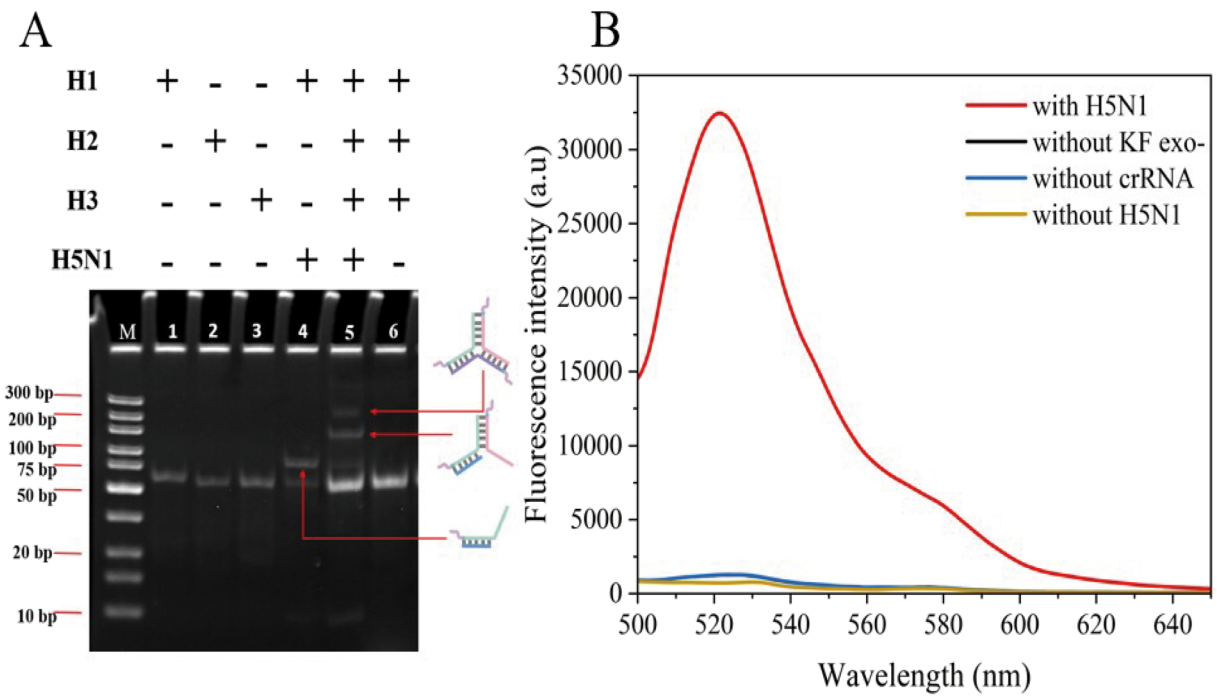

Fig. 1 Feasibility of the proposed method. (A) PAGE verification of feasibility. (M: DNA marker. Lane1: H1. Lane 2: H2. Lane 3: H3. Lane 4: H1 + H5N1 DNA. Lane 5: H1 + H2 + H3 + H5N1 DNA. Lane 6: H1 + H2 + H3); (B) The fluorescence spectra based on CRISPR/Cas12a for H5N1 DNA detection. (With H5N1: all of them. Without KF *exo*-: just no KF, everything else. Without crRNA: just no crRNA, everything else. Without H5N1: just no H5N1 DNA, everything else).

unopened H2 in the H5N1 DNA/H1/H2 complex, indicating successful formation of the three-way junction (TWJ) structures. In contrast, incubation of H1, H2, and H3 without H5N1 DNA did not produce any new bands (lane 6), confirming the stability of the hairpins and demonstrating that the SDA process is specifically triggered by the presence of H5N1 DNA.

The PAGE results strongly support the notion that the TWJ is initiated only in the presence of the target H5N1 DNA, highlighting the specificity of the assay. This conclusion is further corroborated by fluorescence analysis, as illustrated in Fig. 1B. In the experimental group (red line), the addition of 2 nM H5N1 DNA in a 200 μL final reaction volume led to a

significant increase in fluorescence intensity compared to the control group (yellow line). In the whole reaction system, only the absence of crRNA (blue line) or KF *exo-* (black line), other reagents unchanged, negligible fluorescence signals were detected, indicating that both the assembly of the Cas12a protein with crRNA and the presence of KF *exo-* are crucial for initiating the trans-cleavage activity of CRISPR/Cas12a. The involvement of KF *exo-* specifically enhances the fluorescent signal by facilitating strand displacement and amplification.

3.3 Optimization of the CRISPR/Cas12a system

To optimize the performance of the CRISPR/Cas12a system for quantitative detection, the concentration of crRNA was investigated.[52] It was determined that a concentration of 5 nM LbCas12a protein per reaction, combined with varying concentrations of crRNA, formed protein-crRNA complexes optimally, resulting in a fluorescence plateau within the range of 5 to 20 nM crRNA (Fig. 2A). Fluorescence significantly decreased at crRNA concentrations above 20 nM, which was attributed to excess crRNA binding to the activator, thereby reducing the availability of the activated LbCas12a/crRNA complex. Consequently, 5 nM was selected as the optimal crRNA concentration. Subsequent experiments using this optimized crRNA concentration showed that fluorescence reached a plateau at Cas12a concentrations greater than 10 nM (Fig. 2C). Similarly, fluorescence intensity increased as the recombinant RNase inhibitor (RRI) concentration ranged from 0.25 to 1 U, but decreased beyond 1 U (Fig. 2D). The reaction time was also optimized, with peak fluorescence observed after 35 minutes (Fig. 2B). Therefore, the optimal conditions for the reaction were determined to be a crRNA concentration of 5 nM, a Cas12a concentration of 10 nM, 1 U of RRI, and a reaction time of 35 minutes.

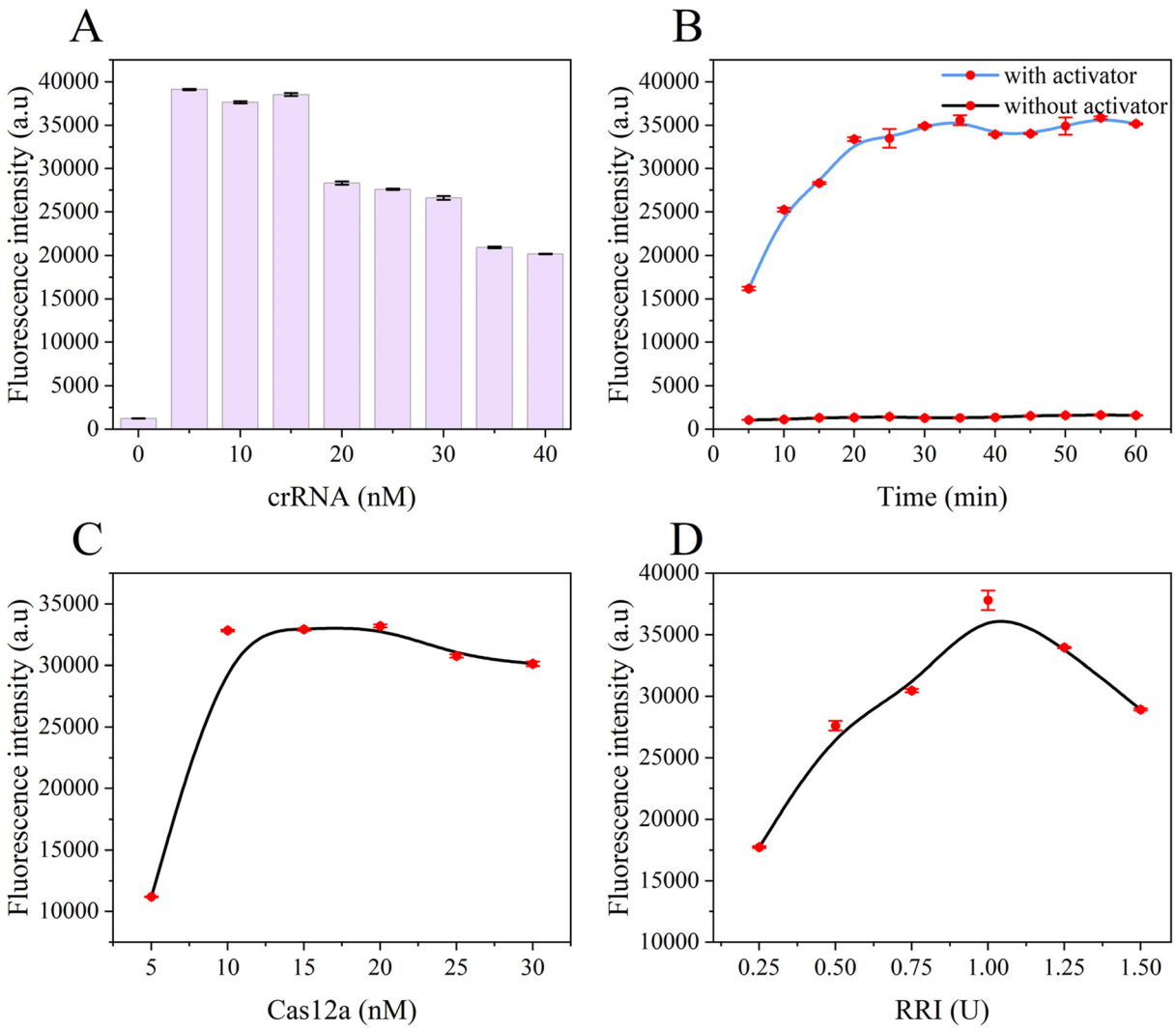

Fig. 2 In a 200 μL system, the effect of reaction conditions on the fluorescence signal. (A) crRNA concentration; (B) reaction time; (C) Cas12a concentration; (D) RRI concentration. Data are expressed as mean ± SD (n = 3).

3.4 Optimization of detection conditions

When comparing the stepwise three-hairpin reaction in cycle 1 with the one-pot reaction, as demonstrated in Fig. 3, enzyme concentration-dependent fluorescence was observed to increase with the concentrations of KF polymerase and Nt. BbvCI endonuclease. Optimized concentrations for polymerase and endonuclease were 0.5 U and 1.5 U (Fig. 3A and B), respectively, in the stepwise reaction and 0.4 U and 1.7 U in the one-pot reaction (Fig. 3C and D). Background signals were significant in both the cycle 2 reaction time exceeding 40 minutes and the cycle 1 reaction time of 16 minutes per step (Fig. S2A and B†), but were absent in the one-pot reaction with cycle 2 at 30 minutes and cycle 1 at 40 minutes (Fig. S2C and D†), hence the choice for subsequent experiments (Fig. S2†). Furthermore, a plateau was reached six minutes after the inactivation time of cycle 2 (Fig. S3A†). A 1 : 1 : 1 ratio of hairpin H1 : H2 : H3 was determined to be optimal in cycle 1, as a disparity significantly decreased fluorescence (Fig. S3B†).

3.5 Sensitivity of H5N1 DNA detection

Under optimized conditions, the sensitivity of the biosensor was evaluated across a range of H5N1 DNA concentrations. As shown in Fig. 4, there is a clear positive correlation between H5N1 DNA concentration and fluorescence intensity, demonstrating the reliability of the biosensor for quantitative detection. Two distinct linear relationships were established: one within the range of 900 fM to 800 pM (Fig. 4C), represented by the equation $F = 19.65767 \times C + 2717.42837$ ($R^2 = 0.9921$), and another in the range of 100 fM to 900 fM (Fig. 4D), represented by the equation $F = 2.61357 \times C + 994.75328$ ($R^2 = 0.9855$). The calculation formula LOD = $3\sigma/k$ according to the 3σ rule,[2] where σ was the standard deviation of 11 blank samples, k was the slope, and the detection limit was calculated to be 72.87

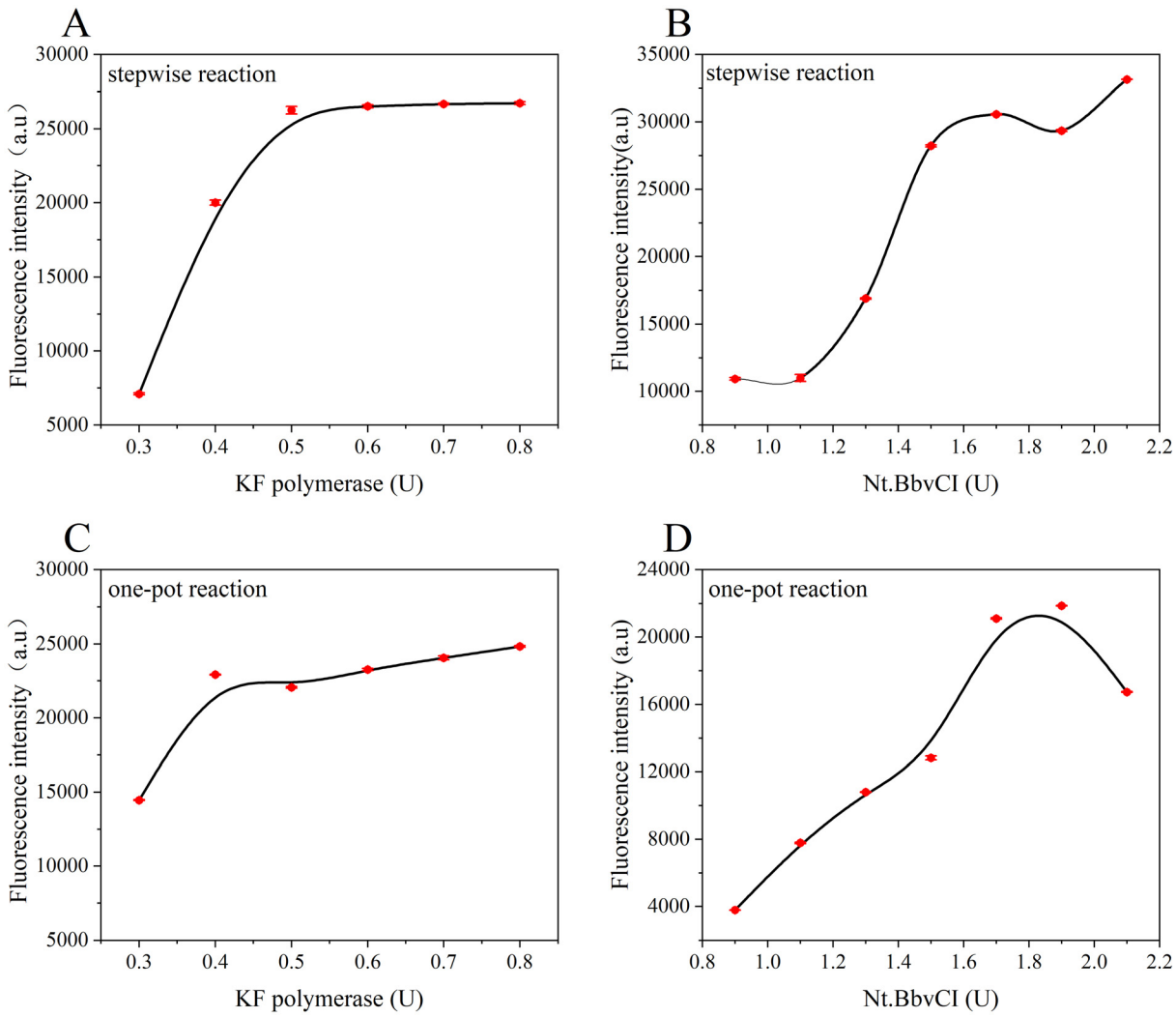

Fig. 3 In a 200 μL system, the effect of reaction conditions on the fluorescence signal. (A) KF polymerase concentration in stepwise reaction; (B) Nt. BbvCI concentration in stepwise reaction; (C) KF polymerase concentration in one-pot reaction; (D) Nt.BbvCI concentration in one-pot reaction. Data are expressed as mean ± SD (n = 3).

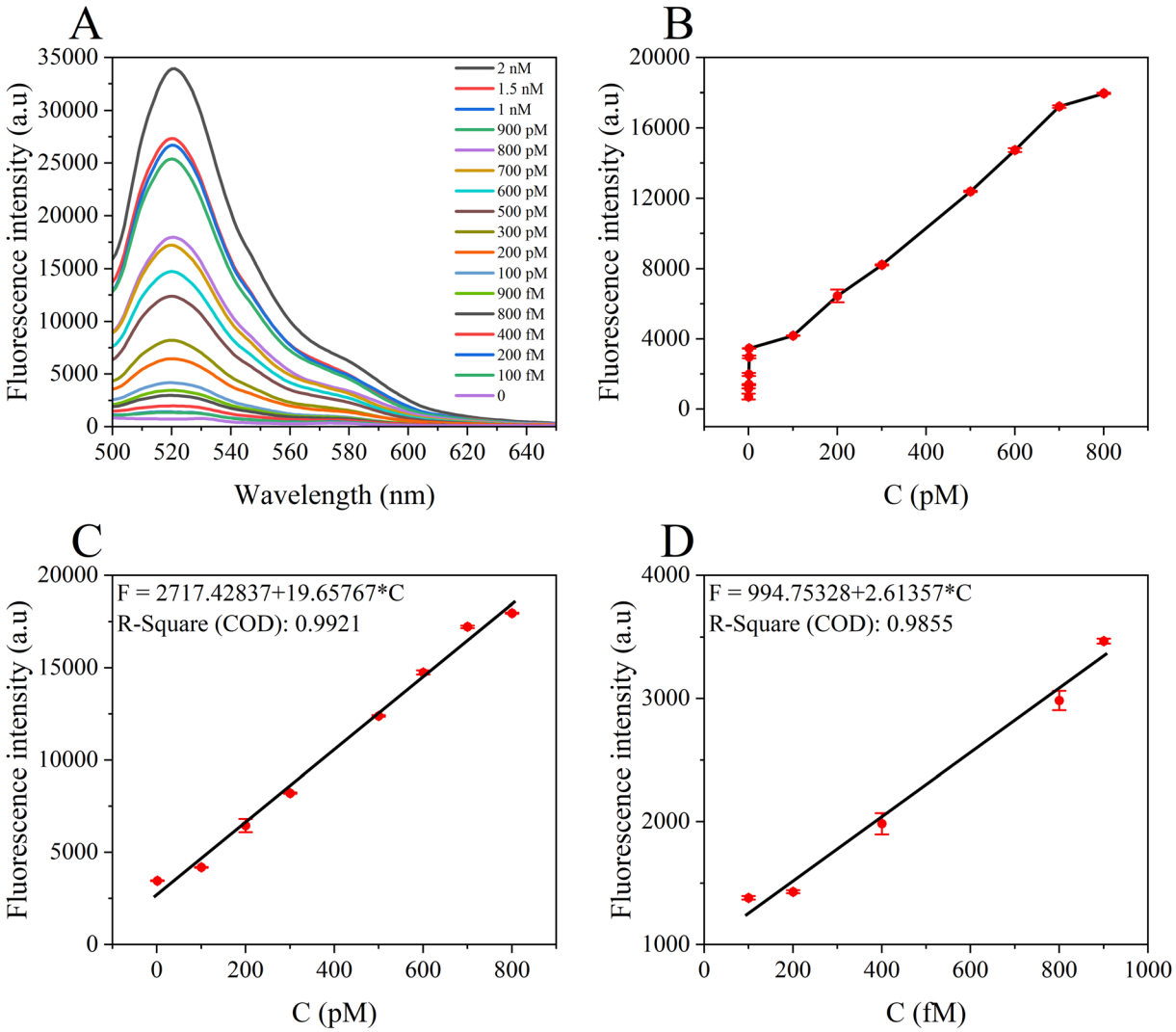

Fig. 4 (A) Fluorescence spectra of H5N1 DNA at different concentrations (0–2 nM). (B) The corresponding curve in the range of 0 to 800 pM for H5N1 DNA detection. (C) The linear calibration curves of 900 fM to 800 pM and (D) 100 fM to 900 fM. Data are expressed as mean ± SD (n = 3).

fM. This low detection limit underscores the method's sensitivity, which is crucial for detecting low concentrations of H5N1, especially in early-stage infections.

The advantages of this biosensor, including its low detection limit, wide linear range, high sensitivity, and excellent selectivity, are largely attributed to its strategic design. The use of three hairpin structures (H1, H2, and H3) with several base tails at their 3′ ends prevents the aggregation of hairpins and non-specific cleavage, ensuring stability and efficient formation of the three-way junctions. Furthermore, the multi-directional chain replacement amplification used in this biosensor results in the production of numerous activators, leading to enhanced signal amplification. The CRISPR/Cas12a system, known for its highly specific target recognition and trans-cleavage activity, further boosts the detection sensitivity and specificity by generating a strong fluorescence response only when the target is present.

Table 1 provides a comparative analysis of the performance of the proposed biosensor with other methods for detecting H5N1 DNA. Compared to previous fluorescence-based techniques, such as those with detection limits of 60 pM,[1] 7.5 pM,[2] 90 pM,[3] and 500 pM,[4] the proposed biosensor demonstrates a significantly lower detection limit of 72.87 fM. This represents a substantial improvement in sensitivity, allowing for the detection of minute quantities of H5N1 DNA that would be undetectable with other existing methods. Additionally, the linear range of the proposed method (100 fM to 800 pM) is broader than many of the previously reported methods, providing greater flexibility for quantifying different concentrations of the target DNA in various sample types. In addition, the biosensing strategy combined with CRISPR/Cas12a and SDA designed by us has low cost of reagents and equipment, simple operation, and can detect the presence of targets in about 2 hours. The TWJ is formed in one pot with less stepwise operation process, and the requirements for equipment in field application are low, which is expected to be tested clinically in the future.

Table 1 Comparison of several methods for detecting DNA

Methods	Target	Linear range	Detection limit	Ref.
Fluorescence	H5N1 DNA	0.2–20 nM	60 pM	1
Fluorescence	H5N1 DNA	0.01–2.5 nM	7.5 pM	2
Fluorescence	H5N1 DNA	0.1–50 nM	90 pM	3
Fluorescence	H5N1 DNA	500 pM–2 μM	500 pM	4
Fluorescence	H5N1 DNA	900 fM–800 pM and 100 fM–900 fM	72.87 fM	This work

The key differentiators of this biosensor, as demonstrated in Table S2,† include not only its superior sensitivity but also its robustness and reliability in complex biological matrices such as serum. Many traditional methods suffer from high background noise and limited applicability to real samples due to non-specific interactions and insufficient amplification efficiency. In contrast, the combination of SDA with CRISPR/Cas12a's collateral cleavage provides a dual amplification mechanism, enhancing both the specificity and the signal-to-noise ratio of the assay. This dual mechanism ensures that the biosensor is capable of discriminating the target from closely related sequences, reducing the likelihood of false positives.

The multi-directional strand displacement amplification plays a crucial role in increasing the number of activators, which in turn maximizes the signal generated by the CRISPR/Cas12a system. Compared to other detection strategies, this

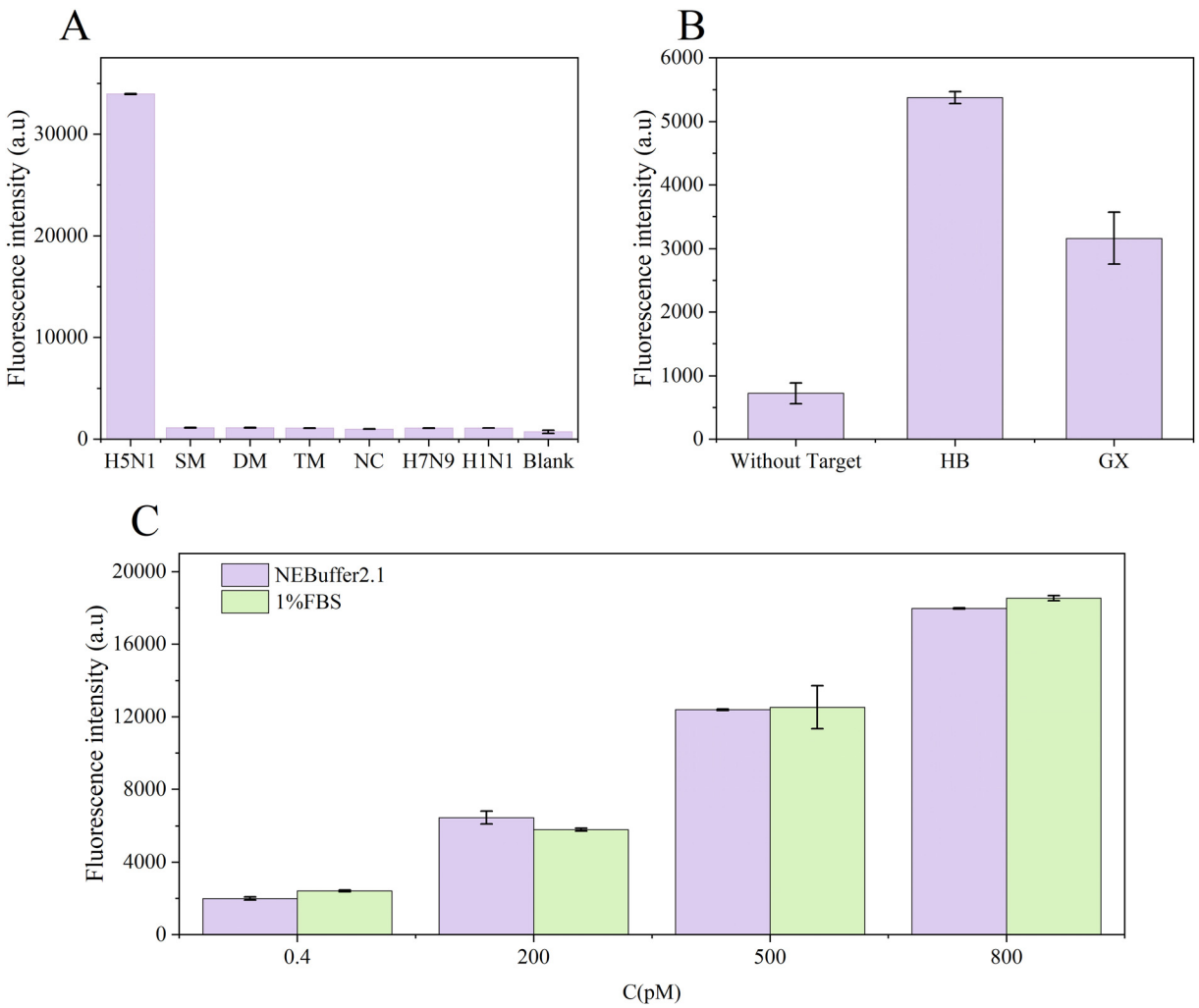

Fig. 5 (A) Selectivity of the method towards H5N1 DNA. The concentration of target, single-base mismatched (SM), double-bases mismatched (DM), three bases mismatched (TM) and non-complementary (NC), H7N9, H1N1 DNA was both 2 nM and the control group (buffer instead of target). (B) The method was tested in actual virus samples. HB (TCID50 = 5.38, Hubei, China) and GX (TCID50 = 5.25, Guangxi, China). Data are expressed as mean ± SD (n = 3). (C) H5N1 DNA test results in buffer (purple) and fetal bovine serum (FBS) samples (green). Data are expressed as mean ± SD (n = 3).

amplification approach, coupled with CRISPR's specificity, in the future, devices for reading fluorescence signals will be miniaturized. For example, Wang *et al.* developed a SCOPE platform,[53] which saves time and is suitable for field use through simplified procedures performed by miniature wireless devices, makes the proposed method particularly powerful for real-world applications, where sensitivity, precision, and robustness are of utmost importance. Overall, the results illustrate that the proposed biosensor provides a highly competitive and effective alternative for H5N1 detection, offering improvements in sensitivity, selectivity, and applicability over existing methods.

3.6 Specific detection of H5N1 DNA

To further ascertain the specificity of the scheme, several mismatched bases and avian influenza virus subtypes were detected alongside the target H5N1 DNA at 2 nM. Non-target DNA groups exhibited negligible fluorescence responses, while H5N1 DNA presence resulted in a significant fluorescence increase (Fig. 5A). This indicates that only H5N1 DNA can open the hairpin H1 to form a subsequent TWJ structure, and the amplified product further stimulates the trans-cleavage activity of CRISPR/Cas12a and sends out a fluorescent signal. In short, the constructed biosensor can detect the target specifically and has good anti-interference ability.

3.7 Detection of H5N1 DNA in FBS

The functionality of the system was tested in fetal bovine serum (FBS) to assess its efficacy in a complex biological matrix. As shown in Fig. 5C, the fluorescence response in serum samples was comparable to that in buffer systems, confirming the system's efficient signal gain in diverse media. The recovery rate of H5N1 DNA in serum was greater than 78.09% and less than 135%, the highest recovery was 135% and the lowest recovery was 78.09%, which may be affected by the uniformity of H5N1 DNA in serum and the experimental procedure. If there is a large difference between the H5N1 DNA background value and the standard serum addition value, the difference between H5N1 DNA and the H5N1 DNA content in serum may be inaccurate, and the recovery rate may be too high or too low due to the many steps of the labeled recovery experiment, with a relative standard deviation below 10%, reinforcing the reliability of the system circuitry for quantitative analysis in complex environments (Table S2†).

3.8 Application to real samples

As shown in Fig. 5B, the fluorescence signal of the detected HB sample (TCID50 = 5.38, Hubei, China) was approximately 10 times that of the without target group and that of the GX sample (TCID50 = 5.25, Guangxi, China) group was approximately 6 times that of the without target group, the inconsistent fluorescence between the two groups may be due to the fact that H5N1 is an RNA virus and is susceptible to RNA enzymes as well as environmental factors, indicating that the method can be applied to the actual sample.

4. Conclusions

We have developed a novel biosensor that combines the principles of strand displacement amplification and CRISPR/Cas12a technology for the highly sensitive detection of H5N1 DNA. The unique design leverages three hairpin structures and the precise target recognition capabilities of the CRISPR/Cas12a system, resulting in a detection platform that exhibits exceptional sensitivity, with a detection limit as low as 72.87 fM, and a broad linear detection range. The biosensor's performance was validated under various conditions, demonstrating its effectiveness in both controlled and complex biological samples, such as serum. The use of three metastable hairpin structures prevents non-specific reactions and ensures efficient production of activators. However, when the biosensor forms TWJ, there will be a non-specific reaction. Subsequent studies will continue on how to reduce this non-specific reaction to improve the stability and detection efficiency of the sensor, while the CRISPR/Cas12a system provides the specificity needed for selective target cleavage and fluorescence signal generation. These features collectively contribute to the biosensor's excellent analytical sensitivity and reliability. Compared to existing methods for H5N1 detection, the biosensor stands out due to its rapid response time, low detection limit, and the potential for point-of-care diagnostics, particularly in resource-limited environments. Its ability to perform well in complex biological matrices further highlights its utility in real-world applications, making it a promising tool for early diagnosis and outbreak monitoring. Future studies could explore the adaptability of this biosensor to other infectious agents by modifying the target-specific sequences. Additionally, efforts to miniaturize and integrate this biosensor into portable devices could facilitate its use in field settings for rapid, on-site detection. Overall, the biosensor presents a versatile and powerful approach for pathogen detection, with significant implications for public health and infectious disease management.

Author contributions

Zhengjiang Wu: conceptualization, methodology, formal analysis, conducting experiments, writing – original draft, writing – review & editing. Jingwen Li: formal analysis, validation. Tao Zhang: formal analysis, writing – review & editing. Kai Zhang: formal analysis, writing – review & editing. Xiaomei Liu: methodology, formal analysis. Zhan Yang: formal analysis, real sample assay. Li Xu: formal analysis, supervision. Kun Han: supervision, writing – review & editing, project administration, funding acquisition.

Data availability

The data are available from the corresponding author on reasonable request.

Conflicts of interest

There are no conflicts to declare.

Acknowledgements

This work was supported by the Strategic Priority Research Program of Chinese Academy of Sciences, "333 High-level Talents Training Project of Jiangsu Province", CAS Key Laboratory of Bio-medical Diagnostics (No: A2023T003), and Natural Science Foundation of Shandong Province (ZR2022QF051).

References

1 Y. Li, C. Liu, Q. Si, T. Jiao, Q. Chen, X. Chen, Q. Chen and J. Wei, Construction of an autocatalysis-driven DNA circuit for highly efficient detection of H5N1 oligonucleotide, *Sens. Actuators, B*, 2023, **394**, 134393, DOI: **10.1016/j.snb.2023.134393**.

2 R. Zou, S. Wang, C. Chen, X. Chen, H. Gong and C. Cai, An enzyme-free DNA circuit-assisted MoS2 nanosheet enhanced fluorescence assay for label-free DNA detection, *Talanta*, 2021, **222**, 121505, DOI: **10.1016/j.talanta.2020.121505**.

3 X. Zhao, Z. Zhu, R. Zou, L. Wang, H. Gong and C. Cai, An enzyme-free three-dimensional DNA walker powered by catalytic hairpin assembly for H5N1 DNA ratiometric detection, *Microchem. J.*, 2021, **170**, 106728, DOI: **10.1016/j.microc.2021.106728**.

4 Y. Zhang, F. Mu, Y. Duan, Q. Li, Y. Pan, H. Du, P. He, X. Shen, Z. Luo, C. Zhu and L. Wang, Label-Free Analysis of H5N1 Virus Based on Three-Segment Branched DNA-Templated Fluorescent Silver Nanoclusters, *ACS Appl. Mater. Interfaces*, 2020, **12**(43), 48357–48362, DOI: **10.1021/acsami.0c14509**.

5 H. Gong, S. Chen, L. Tang, F. Chen, C. Chen and C. Cai, Ultra-Sensitive Portable Visual Paper-Based Viral Molecularly Imprinted Sensor without Autofluorescence Interference, *Anal. Chem.*, 2023, **95**(48), 17691–17698, DOI: **10.1021/acs.analchem.3c03506**.

6 G. Hang, X. Luru, L. Yong, P. Tao, C. Chunyan, C. Feng and C. Changqun, Self-service aptamer-free molecularly imprinted paper-based sensor for high-sensitivity visual detection of influenza H5N1, *Analyst*, 2025, **150**, 552–558, DOI: **10.1039/d4an01233j**.

7 H. Gong, L. Tang, C. Chen, F. Chen and C. Cai, Portable paper-based molecularly imprinted sensor for visual real-time detection of influenza virus H5N1, *Chem. Eng. J.*, 2023, **477**, 146990, DOI: **10.1016/j.cej.2023.146990**.

8 J. Lin, R. Wang, P. Jiao, Y. Li, Y. Li, M. Liao, Y. Yu and M. Wang, An impedance immunosensor based on low-cost microelectrodes and specific monoclonal antibodies for rapid detection of avian influenza virus H5N1 in chicken swabs, *Biosens. Bioelectron.*, 2015, **67**, 546–552, DOI: **10.1016/j.bios.2014.09.037**.

9 F. Shisong, L. Jianxiong, C. Xiaowen, Z. Cunyou, W. Ting, L. Xing, W. Xin, W. Chunli, Z. Renli, C. Jinquan, X. Hong and Y. Muhua, Simultaneous detection of influenza virus type B and influenza A virus subtypes H1N1, H3N2, and H5N1 using multiplex real-time RT-PCR, *Appl. Microbiol. Biotechnol.*, 2011, **90**(4), 1463–1470, DOI: **10.1007/s00253-011-3192-8**.

10 Y. T. Kim, J. H. Jung, Y. K. Choi and T. S. Seo, A packaged paper fluidic-based microdevice for detecting gene expression of influenza A virus, *Biosens. Bioelectron.*, 2014, **61**, 485–490, DOI: **10.1016/j.bios.2014.06.006**.

11 H. Gong, G. Cai, Y. Li, N. Jiang, C. Chen, F. Chen and C. Cai, Portable dual-function ratio-type triple-emission molecularly imprinted fluorescence sensor for the simultaneous visual detection of hepatitis A and B viruses, *Anal. Chim. Acta*, 2025, **1336**, 343451, DOI: **10.1016/j.aca.2024.343451**.

12 H. Bai, R. Wang, B. Hargis, H. Lu and Y. Li, A SPR Aptasensor for Detection of Avian Influenza Virus H5N1, *Sensors*, 2012, **12**(9), 12506–12518, DOI: **10.3390/s120912506**.

13 Y. Tan, Q. Ng, Q. Jia, J. Kwang, F. He and R. M. Sandri-Goldin, A Novel Humanized Antibody Neutralizes H5N1 Influenza Virus via Two Different Mechanisms, *J. Virol.*, 2015, **89**(7), 3712–3722, DOI: **10.1128/jvi.03014-14**.

14 X. Xiao, Z. Lin, X. Huang, J. Lu, Y. Zhou, L. Zheng and Y. Lou, Rapid and Sensitive Detection of Vibrio vulnificus Using CRISPR/Cas12a Combined With a Recombinase-Aided Amplification Assay, *Front. Microbiol.*, 2021, **12**, 767315, DOI: **10.3389/fmicb.2021.767315**.

15 W. Feng, H. Peng, J. Xu, Y. Liu, K. Pabbaraju, G. Tipples, M. A. Joyce, H. A. Saffran, D. L. Tyrrell, S. Babiuk, H. Zhang and X. C. Le, Integrating Reverse Transcription Recombinase Polymerase Amplification with CRISPR Technology for the One-Tube Assay of RNA, *Anal. Chem.*, 2021, **93**(37), 12808–12816, DOI: **10.1021/acs.analchem.1c03456**.

16 J. Xu, J. Ma, Y. Li, L. Kang, B. Yuan, S. Li, J. Chao, L. Wang, J. Wang, S. Su and Y. Yuan, A general RPA-CRISPR/Cas12a sensing platform for Brucella spp. detection in blood and milk samples, *Sens. Actuators, B*, 2022, **364**, 131864, DOI: **10.1016/j.snb.2022.131864**.

17 M. Zhou, H. Wang, C. Li, C. Yan, P. Qin and L. Huang, CRISPR/Cas9 mediated triple signal amplification platform for high selective and sensitive detection of single base mutations, *Anal. Chim. Acta*, 2022, **1230**, 340421, DOI: **10.1016/j.aca.2022.340421**.

18 X. Ke, Y. Ou, Y. Lin and T. Hu, Enhanced chemiluminescence imaging sensor for ultrasensitive detection of nucleic acids based on HCR-CRISPR/Cas12a, *Biosens. Bioelectron.*, 2022, **212**, 114428, DOI: **10.1016/j.bios.2022.114428**.

19 Y. Yang, T. Wu, L. P. Xu and X. Zhang, Portable detection of Staphylococcus aureus using personal glucose meter based on hybridization chain reaction strategy, *Talanta*, 2021, **226**, 122132, DOI: **10.1016/j.talanta.2021.122132**.

20 M. Li, N. Luo, X. Liao and L. Zou, Proximity hybridization-regulated CRISPR/Cas12a-based dual signal amplification

strategy for sensitive detection of circulating tumor DNA, *Talanta*, 2023, **257**, 124395, DOI: 10.1016/j.talanta.2023.124395.

21 H. Gong, S. Yao, Y. Li, C. Chen, F. Chen and C. Cai, Combined detection of hepatitis B virus surface antigen and hepatitis B virus DNA using a DNA sensor, *Anal. Methods*, 2024, **16**(43), 7319–7324, DOI: 10.1039/d4ay01629g.

22 K. Abnous, A. K. Abdolabadi, M. Ramezani, M. Alibolandi, M. A. Nameghi, T. Zavvar, Z. Khoshbin, P. Lavaee, S. M. Taghdisi and N. M. Danesh, A highly sensitive electrochemical aptasensor for cocaine detection based on CRISPR-Cas12a and terminal deoxynucleotidyl transferase as signal amplifiers, *Talanta*, 2022, **241**, 123276, DOI: 10.1016/j.talanta.2022.123276.

23 C. Lin, H. Zheng, Y. Huang, Z. Chen, F. Luo, J. Wang, L. Guo, B. Qiu, Z. Lin and H. Yang, Homogeneous electrochemical aptasensor for mucin 1 detection based on exonuclease I-assisted target recycling amplification strategy, *Biosens. Bioelectron.*, 2018, **117**, 474–479, DOI: 10.1016/j.bios.2018.06.056.

24 H. E. Zumrut, S. Batool, K. V. Argyropoulos, N. Williams, R. Azad and P. R. Mallikaratchy, Integrating Ligand-Receptor Interactions and In Vitro Evolution for Streamlined Discovery of Artificial Nucleic Acid Ligands, *Mol. Ther.–Nucleic Acids*, 2019, **17**, 150–163, DOI: 10.1016/j.omtn.2019.05.015.

25 X. Zhao, Z. Wang, B. Yang, Z. Li, Y. Tong, Y. Bi, Z. Li, X. Xia, X. Chen, L. Zhang, W. Wang and G. Y. Tan, Integrating PCR-free amplification and synergistic sensing for ultrasensitive and rapid CRISPR/Cas12a-based SARS-CoV-2 antigen detection, *Synth. Syst. Biotechnol.*, 2021, **6**(4), 283–291, DOI: 10.1016/j.synbio.2021.09.007.

26 S. Xu, S. Wang, L. Guo, Y. Tong, L. Wu and X. Huang, Nanozyme-catalysed CRISPR-Cas12a system for the preamplification-free colorimetric detection of lead ion, *Anal. Chim. Acta*, 2023, **1243**, 340827, DOI: 10.1016/j.aca.2023.340827.

27 J. Li, W. Zhou, R. Yuan and Y. Xiang, Aptamer proximity recognition-dependent strand translocation for enzyme-free and amplified fluorescent detection of thrombin via catalytic hairpin assembly, *Anal. Chim. Acta*, 2018, **1038**, 126–131, DOI: 10.1016/j.aca.2018.07.011.

28 H. Sun, S. Zhou, Y. Liu, P. Lu, N. Qi, G. Wang, M. Yang, D. Huo and C. Hou, A fluorescent biosensor based on exponential amplification reaction-initiated CRISPR/Cas12a (EIC) strategy for ultrasensitive DNA methyltransferase detection, *Anal. Chim. Acta*, 2023, **1239**, 340732, DOI: 10.1016/j.aca.2022.340732.

29 L. Xu, Q. Dai, Z. Shi, X. Liu, L. Gao, Z. Wang, X. Zhu and Z. Li, Accurate MRSA identification through dual-functional aptamer and CRISPR-Cas12a assisted rolling circle amplification, *J. Microbiol. Methods*, 2020, **173**, 105917, DOI: 10.1016/j.mimet.2020.105917.

30 W. Ma, M. Liu, S. Xie, B. Liu, L. Jiang, X. Zhang and X. Yuan, CRISPR/Cas12a system responsive DNA hydrogel for label-free detection of non-glucose targets with a portable personal glucose meter, *Anal. Chim. Acta*, 2022, **1231**, 340439, DOI: 10.1016/j.aca.2022.340439.

31 M. Liu, W. Ma, Y. Zhou, B. Liu, X. Zhang and S. Zhang, A Label-Free Photoelectrochemical Biosensor Based on CRISPR/Cas12a System Responsive Deoxyribonucleic Acid Hydrogel and "Click" Chemistry, *ACS Sens.*, 2022, **7**(10), 3153–3160, DOI: 10.1021/acssensors.2c01636.

32 Z. Lv, Q. Wang and M. Yang, Multivalent Duplexed-Aptamer Networks Regulated a CRISPR-Cas12a System for Circulating Tumor Cell Detection, *Anal. Chem.*, 2021, **93**(38), 12921–12929, DOI: 10.1021/acs.analchem.1c02228.

33 H. Chen, Z. Zhuang, Y. Chen, C. Qiu, Y. Qin, C. Tan, Y. Tan and Y. Jiang, A universal platform for one-pot detection of circulating non-coding RNA combining CRISPR-Cas12a and branched rolling circle amplification, *Anal. Chim. Acta*, 2023, **1246**, 340896, DOI: 10.1016/j.aca.2023.340896.

34 H. Zhang, S. Yao, R. Sheng, J. Wang, H. Li, Y. Fu, J. Li, X. Zhang and C. Zhao, A cascade amplification strategy for ultrasensitive Salmonella typhimurium detection based on DNA walker coupling with CRISPR-Cas12a, *J. Colloid Interface Sci.*, 2022, **625**, 257–263, DOI: 10.1016/j.jcis.2022.06.027.

35 X. Wang, X. Mu, J. Li, G. Liu, S. Zhao and J. Tian, A novel nanoparticle surface-constrained CRISPR-Cas12a 3D DNA walker-like nanomachines for sensitive and stable miRNAs detection, *Anal. Chim. Acta*, 2023, **1251**, 340950, DOI: 10.1016/j.aca.2023.340950.

36 K. S. Makarova, Y. I. Wolf, J. Iranzo, S. A. Shmakov, O. S. Alkhnbashi, S. J. J. Brouns, E. Charpentier, D. Cheng, D. H. Haft, P. Horvath, S. Moineau, F. J. M. Mojica, D. Scott, S. A. Shah, V. Siksnys, M. P. Terns, Č. Venclovas, M. F. White, A. F. Yakunin, W. Yan, F. Zhang, R. A. Garrett, R. Backofen, J. van der Oost, R. Barrangou and E. V. Koonin, Evolutionary classification of CRISPR–Cas systems: a burst of class 2 and derived variants, *Nat. Rev. Microbiol.*, 2019, **18**(2), 67–83, DOI: 10.1038/s41579-019-0299-x.

37 Z. Chi, Y. Wu, L. Chen, H. Yang, M. R. Khan, R. Busquets, N. Huang, X. Lin, R. Deng, W. Yang and J. Huang, CRISPR-Cas14a-integrated strand displacement amplification for rapid and isothermal detection of cholangiocarcinoma associated circulating microRNAs, *Anal. Chim. Acta*, 2022, **1205**, 339763, DOI: 10.1016/j.aca.2022.339763.

38 G. Cao, Y. Deng, X. Chen, D. Huo, J. Li, M. Yang and C. Hou, The fluorescent biosensor for detecting N(6) methyladenine FzD5 mRNA and MazF activity, *Anal. Chim. Acta*, 2021, **1188**, 339185, DOI: 10.1016/j.aca.2021.339185.

39 S. Zhou, H. Sun, D. Huo, X. Wang, N. Qi, L. Peng, M. Yang, P. Lu and C. Hou, A novel methyl-dependent DNA endonuclease GlaI coupling with double cascaded strand displacement amplification and CRISPR/Cas12a for ultra-sensitive detection of DNA methylation, *Anal. Chim. Acta*, 2022, **1212**, 339914, DOI: 10.1016/j.aca.2022.339914.

40 X. Wang, Y. Qin, Y. Huang, K. Hu, S. Zhao and J. Tian, A sensitive and facile microRNA detection based on

CRISPR-Cas12a coupled with strand displacement amplification, *Spectrochim. Acta, Part A*, 2022, **279**, 121476, DOI: **10.1016/j.saa.2022.121476**.

41 Y. Liu, S. Zhou, H. Sun, J. Dong, L. Deng, N. Qi, Y. Wang, D. Huo and C. Hou, Ultrasensitive fluorescent biosensor for detecting CaMV 35S promoter with proximity extension mediated multiple cascade strand displacement amplification and CRISPR/Cpf 1, *Anal. Chim. Acta*, 2022, **1215**, 339973, DOI: **10.1016/j.aca.2022.339973**.

42 H. Shivram, B. F. Cress, G. J. Knott and J. A. Doudna, Controlling and enhancing CRISPR systems, *Nat. Chem. Biol.*, 2020, **17**(1), 10–19, DOI: **10.1038/s41589-020-00700-7**.

43 J. Strecker, S. Jones, B. Koopal, J. Schmid-Burgk, B. Zetsche, L. Gao, K. S. Makarova, E. V. Koonin and F. Zhang, Engineering of CRISPR-Cas12b for human genome editing, *Nat. Commun.*, 2019, **10**, 212, DOI: **10.1038/s41467-018-08224-4**.

44 M. Naeem, S. Majeed, M. Z. Hoque and I. Ahmad, Latest Developed Strategies to Minimize the Off-Target Effects in CRISPR-Cas-Mediated Genome Editing, *Cells*, 2020, **9**(7), 1608, DOI: **10.3390/cells9071608**.

45 P. An, B. Luo, X. Zhan, Y. Jiang, F. Lan and Y. Wu, CRISPR/Cas12a bio-assay integrated with metal-organic framework based enhanced fluorescent labels for ultrasensitive detection of circulating tumor DNA, *Sens. Actuators, B*, 2023, **383**, 133623, DOI: **10.1016/j.snb.2023.133623**.

46 Y. Yang, W. Yi, F. Gong, Z. Tan, X. Shan, J. Qian, C. Xie, X. Ji, Z. Zheng and Z. He, An all-in-one assay based on CRISPR/Cas13a and a DNA circuit for rapid and ultrasensitive detection of Echovirus 11, *Sens. Actuators, B*, 2023, **388**, 133851, DOI: **10.1016/j.snb.2023.133851**.

47 P. Wu, X. Ye, D. Wang, F. Gong, X. Wei, S. Xiang, J. Zhang, T. Kai and P. Ding, A novel CRISPR/Cas14a system integrated with 2D porphyrin metal-organic framework for microcystin-LR determination through a homogeneous competitive reaction, *J. Hazard. Mater.*, 2022, **424**(Pt D), 127690, DOI: **10.1016/j.jhazmat.2021.127690**.

48 J. Xu, X. Bai, X. Zhang, B. Yuan, L. Lin, Y. Guo, Y. Cui, J. Liu, H. Cui, X. Ren, J. Wang and Y. Yuan, Development and application of DETECTR-based rapid detection for pathogenic Bacillus anthracis, *Anal. Chim. Acta*, 2023, **1247**, 340891, DOI: **10.1016/j.aca.2023.340891**.

49 L. B. Harrington, D. Burstein, J. S. Chen, D. Paez-Espino, E. Ma, I. P. Witte, J. C. Cofsky, N. C. Kyrpides, J. F. Banfield and J. A. Doudna, Programmed DNA destruction by miniature CRISPR-Cas14 enzymes, *Science*, 2018, **362**(6416), 839–842, DOI: **10.1126/science.aav4294**.

50 D. Li, S. Ling, H. Wu, Z. Yang and B. Lv, CRISPR/Cas12a-based biosensors for ultrasensitive tobramycin detection with single- and double-stranded DNA activators, *Sens. Actuators, B*, 2022, **355**, 131329, DOI: **10.1016/j.snb.2021.131329**.

51 S.-Y. Li, Q.-X. Cheng, J.-K. Liu, X.-Q. Nie, G.-P. Zhao and J. Wang, CRISPR-Cas12a has both cis- and trans-cleavage activities on single-stranded DNA, *Cell Res.*, 2018, **28**(4), 491–493, DOI: **10.1038/s41422-018-0022-x**.

52 J. S. Chen, E. Ma, L. B. Harrington, M. Da Costa, X. Tian, J. M. Palefsky and J. A. Doudna, CRISPR-Cas12a target binding unleashes indiscriminate single-stranded DNase activity, *Science*, 2018, **360**(6387), 436–439, DOI: **10.1126/science.aar6245**.

53 Y. Wang, H. Chen, K. Lin, Y. Han, Z. Gu, H. Wei, K. Mu, D. Wang, L. Liu, R. Jin, R. Song, Z. Rong and S. Wang, Ultrasensitive single-step CRISPR detection of monkeypox virus in minutes with a vest-pocket diagnostic device, *Nat. Commun.*, 2024, **15**, 3279, DOI: **10.1038/s41467-024-47518-8**.